Application of LQ and IMC Controllers to a Packed-Bed Reactor

A practical application of advanced, model-based, multivariable control to a pilot plant packed-bed reactor carrying out highly exothermic butane hydrogenolysis reactions is presented. The system is first stabilized by using butane flow rate to control the reactor hot-spot temperature. Propane production and butane conversion are then controlled using multivariable controllers that manipulate the hot-spot temperature set point and hydrogen flow rate. The controller designs are based on multivariable transfer function models developed using multivariable time series and process identification methods.

Two types of multivariable controllers are applied. The first is an internal model controller (IMC) utilizing a stabilized approximation of the model inverse and a tunable exponential filter. The second is a linear-quadratic (LQ) controller design using pulse transfer function models to characterize the process dynamics and autoregressive-moving average models to characterize the disturbances. The optimal control solution was arrived at via a spectral factorization solution to the Wiener-Hopf equations. The results indicate that both designs, if well tuned, provide good performance and robustness over a wide range of operation.

D. J. Kozub, J. F. MacGregor
Dept. of Chemical Engineering
McMaster University
Hamilton, Ontario, Canada L8S 4L7

J. D. Wright
Xerox Research Centre
Mississauga, Ontario, Canada

Introduction

An important problem in many chemical processes is that of controlling the product stream compositions from catalytic reactors in which one is carrying out multiple reactions involving multiple species. A high degree of coupling among the product compositions due to the reaction stoichiometry makes the control problem a truly multivariable one. Since the reactions are often highly exothermic and have high activation energies, stability of the reactor is also a major concern. Furthermore, reaction kinetics are usually highly nonlinear in both reactant concentrations and temperature. A controller design strategy for such reactors must therefore be capable of handling complex interactions between input-output pairs, and must be robust to modeling errors and nonlinearities over the operating region.

Advanced optimal controller design using a state space model formulation of the multidimensional problem has received much attention in control literature. Successful application of this theory has been demonstrated by Jutan et al. (1977), Sorensen et al. (1980a,b), and Wallman et al. (1979) to packed-bed control problems using rigorous mechanistic modeling that led to convenient state space model forms. This approach to a packed-bed reactor control problem was also found to be successful by MacGregor and Wong (1980) using empirical transfer function model identification followed by transformation to state space form. Optimal linear-quadratic controller design is usually associated with these state space techniques. However, when one has measured or inferred values of the outputs to be controlled, there are many advantages to designing controllers using input/output transfer function models. The resulting controllers are then expressed directly in terms of past inputs and outputs, and the structure of the controllers is more apparent.

In this paper we present the design and results of practical applications of two multivariable controllers to a pilot plant tubular reactor carrying out the highly exothermic hydrogenolysis of butane over a nickel on silica gel catalyst. A favorable choice of input control variables is demonstrated, which leads to an open-loop stable configuration through use of an internal hot-spot controller. In this work we employ simple linear empirical input/output models developed from time series analysis and process identification techniques on data collected directly from the reactor. The two multivariable designs presented are linear-

Correspondence concerning this paper should be addressed to J. F. MacGregor.

quadratic (LQ) output control and internal model control (IMC). The designs are straightforward for practical chemical process industrial application, and take full advantage of the true interactive nature of a multidimensional system to achieve good controller performance. Furthermore, they allow one to incorporate into the designs a considerable degree of robustness to mismatch between the model and the process.

Multivariable Control

Multivariable model representation

There has been a renewed interest in controller design techniques using multivariable models in pulse transfer function form. However, unlike single-input/single-output designs, multivariable designs are hampered by the noncommuting property of matrices and difficult matrix inversions. A convenient representation for discrete linear multivariable processes is the right matrix fraction form:

$$Y(t) = \omega(z^{-1})\delta(z^{-1})^{-1}z^{-k}U(t) + \theta(z^{-1})\phi(z^{-1})^{-1}A(t) \quad (1)$$

which leads to some simplification in the controller design equations. $Y(t)$ represents the vector of n observable outputs and $U(t)$ a vector of n controllable inputs at sampling interval t. $\omega(z^{-1})$ and $\delta(z^{-1})$ are $(n \times n)$ polynomial matrices in the backward shift operator z^{-1}. $\delta(z^{-1})$ is diagonal with the coefficient of z^0 equal to I. The minimum number of whole periods of delay is given by k.

The second term on the righthand side of Eq. 1 is a model characterizing the nature of the process disturbances. It is an autoregressive integrated moving average (ARIMA) model also expressed in a right matrix fraction form. $\theta(z^{-1})$ and $\phi(z^{-1})$ are $(n \times n)$ polynomial matrices in z^{-1}. The coefficient of z^0 in both matrices is I, and $\phi(z^{-1})$ is diagonal. Nonstationarity of a process disturbance is accounted for by a $(1 - z^{-1})$ factor in the corresponding element of the $\phi(z^{-1})$ matrix. Such models are capable of representing either stochastic or deterministic disturbances and set point changes, depending on the nature of the distribution of the white noise sequence $A(t)$ (MacGregor et al., 1984).

Right matrix fraction representations are not unique. A simple and convenient method for transforming rational transfer function matrices into a right matrix fraction form is by choosing the ith diagonal elements of $\delta(z^{-1})$ or $\phi(z^{-1})$ to be the greatest common factor of the denominators of the ith column of the rational transfer function matrix or ARIMA matrix, respectively.

Linear quadratic control

This section presents the results of the linear quadratic (LQ) optimal control problem using a spectral factorization solution of the Wiener-Hopf equations. Details of the solution are given by Wilson (1970), and Harris and MacGregor (1987), and the structure and properties of these controllers are discussed thoroughly by Harris and MacGregor.

The performance index chosen in the LQ output controller design for square multivariable systems with nonstationary disturbances and set-point change models is the minimization of

$$J = \lim_{N\to\infty} \frac{1}{N} E\left\{\sum_{t=1}^{N} e^T(t)Q_1e(t) + \nabla U^T(t)Q_2\nabla U(t)\right\} \quad (2)$$

where Q_1 and Q_2 are positive semidefinite weighting matrices, $\nabla U(t) = U(t) - U(t-1)$, and $e(t) = Y(t) - Y_{sp}(t)$. The design of these controllers requires the specification of a weighting matrix Q_1 on the output error variances, and a weighting matrix Q_2 on the variance of the changes in the input manipulations. Q_1 is usually chosen to be diagonal, with the magnitude of each diagonal element reflecting the relative importance of a unit change in each output. Q_2 is usually taken to be a diagonal matrix, and is used to tune the controller by adjusting the diagonal elements. Thus one has a single tuning parameter for each input.

Harris and MacGregor (1987) show that the general LQ optimal feedback control solution can be expressed in the internal model controller form:

$$U(t) = H_1(z^{-1})[G_m(z^{-1})U(t) - Y(t)] + H_2(z^{-1})\,Y_{sp}(t) \quad (3)$$

where

$$H_1(z^{-1}) = G_c(z^{-1})\,F_1(z^{-1}) \quad (4)$$

$$H_2(z^{-1}) = G_c(z^{-1})\,F_2(z^{-1}) \quad (5)$$

The control block diagram is shown in Figure 1. $G_m(z^{-1})$ is an $n \times n$ process model transfer function and $Y_{sp}(t)$ is the set point. $G_c(z^{-1})$ is an optimal approximate inverse of the process model given by:

$$G_c(z^{-1}) = \delta(z^{-1})\,\Gamma(z^{-1})^{-1} \quad (6)$$

where $\Gamma(z^{-1})$ is an $n \times n$ nonrational polynomial matrix in z^{-1} having no zeros outside the unit circle. $\Gamma(z^{-1})$ is determined from the solution to the spectral factorization equation

$$\omega^T(z)Q_1\omega(z^{-1}) + \delta^T(z)(1-z)\,Q_2(1-z^{-1})\,\delta(z^{-1}) = \Gamma^T(z)Q_1\Gamma(z^{-1}) \quad (7)$$

The optimal filters $F_i(z^{-1})$ in Eqs. 4 and 5 are determined from

$$F(z^{-1}) = T(z^{-1})\Theta(z^{-1})^{-1} \quad (8)$$

where $T(z^{-1})$, a nonrational polynomial matrix, is determined by solving the Diophantine equation

$$\omega^T(z)z^kQ_1\theta(z^{-1}) = zP(z)\phi(z^{-1}) + \Gamma^T(z)Q_1T(z^{-1}) \quad (9)$$

LQ controllers will always be stable for any choice of input weighting matrices provided no model mismatch is present. When model mismatch is present, stability cannot be guaran-

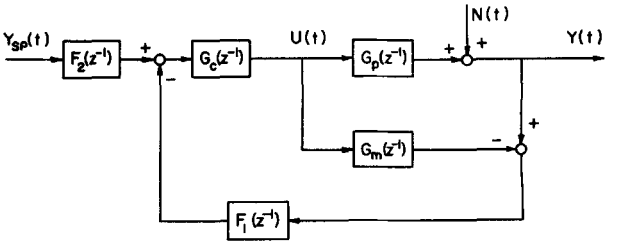

Figure 1. Internal model controller block diagram.

teed for any arbitrary choice of input weighting matrices. However, the robustness of LQ controllers can be greatly enhanced by increasing the magnitude of input penalty weights Q_2 without sacrificing much in the way of performance (Bergh and MacGregor, 1987; Harris and MacGregor, 1987).

Internal model control

In the preceding section it was shown that the LQ controller can be expressed in the internal model control (IMC) structure shown in Figure 1. It is important to note that all model-based controllers can be put in this form. The only difference among these multidimensional model-based controllers is how one chooses the approximate model inverse $G_c(z^{-1})$ and the filters $F_1(z^{-1})$ and $F_2(z^{-1})$. There are infinitely many ways of specifying these terms. It is only necessary that $G_c(z^{-1})$ be stable to ensure closed-loop stability with the nominal model, and that it have no predictive elements. The best choice depends on the nature of the multivariable process and the desired closed-loop performance.

Garcia and Morari (1985a, b) suggested a simple method for selecting $G_c(z^{-1})$ and $F(z^{-1})$ for square systems that leads to a stable, decoupled closed-loop response for the nominal model. In this design the approximate model inverse is given by

$$G_c(z^{-1}) = [\delta(z^{-1})\omega(z^{-1})^{-1}z^{k}]\ V_{+1}(z^{-1})\ V_{+2}(z^{-1}) \quad (10)$$

The first expression in brackets on the righthand side of Eq. 10 is the inverse of the process model. $V_{+1}(z^{-1})$ is a diagonal matrix with each diagonal element in the form $z^{-s(j)}$. This matrix eliminates prediction terms in the inverted process model. The lag element $s(j)$ is equal to k plus the highest positive power of z in column j of the inverted $\omega(z^{-1})$ matrix. This choice of $V_{+1}(z^{-1})$ leads to $s(j)$ periods of delay in the closed-loop response of output j. $V_{+2}(z^{-1})$ is a rational or nonrational polynomial in z^{-1} which removes or replaces unwanted zeros in $|\omega(z^{-1})|$ that will appear in the controller. Zeros of $|\omega(z^{-1})|$ that are outside the unit circle will lead to an unstable controller. The designer can choose to simply cancel unstable zeros or cancel and replace unstable zeros by their image or by any other desired values. Replacement of unstable zeros with their image can be shown to be optimal in a least-squares sense for a decoupled response. Stable zeros of $\omega(z^{-1})$ located near $(-1,0)$ lead to unfavorable input ringing, and should be removed using $V_{+2}(z^{-1})$.

$F_1(z^{-1})$ and $F_2(z^{-1})$ are chosen to be diagonal (decoupled) first-order exponential filters as given below:

$$F(z^{-1}) = \text{diag}\left\{\frac{1-f_{ii}}{1-f_{ii}z^{-1}}\right\} \quad (11)$$

where each filter parameter lies in the range of $0 \le f_{ii} < 1$. One filter factor for each output can be used to shape the closed-loop response (Dahlin controller), or to reduce the severity of input manipulations and improve the robustness of the controller.

Comparisons of controller designs

The differences between the LQ controller design in IMC form and the approach of Garcia and Morari (1985a) are summarized in Table 1. The approximate inverse, $G_c(z^{-1})$, in the LQ design is formed by replacing $z^{-k}\omega(z^{-1})$ of the process model by the spectral factor $\Gamma(z^{-1})$ from Eq. 7. In the second approach, the exact model inverse is formed and then postmultiplied by $V_{+1}(z^{-1})$ and $V_{+2}(z^{-1})$ to obtain a usable inverse. Note that in this latter method the approximate inverse remains fixed during tuning with the filter, $F(z^{-1})$, while in the LQ design tuning with the input weighting matrices affects the approximate model inverse as well as the filter. The choice of $V_{+1}(z^{-1})$ and $V_{+2}(z^{-1})$ has been shown to be very simple for square systems if a completely decoupled closed-loop output response is desired. Holt and Morari (1985a, b) have shown that this decoupled design provides a minimum integral squared error inverse for step set point changes if the multivariable process is invertible and balanced. A multivariable process is balanced if the rows or columns of $G_m(z^{-1})$ can be manipulated such that the minimum dead time in each row appears on the diagonal. Therefore, if these two properties hold for the multivariable process, the decoupled inverse design will be identical to the inverse obtained from the LQ solution with $Q_2 = 0$. High-performance control of an unbalanced multivariable process may not be possible using the decoupled design, especially if there are large differences between the minimum process response times and the decoupled closed-loop output response times. The search for a least-squares optimal inverse is far from trivial when the process is not balanced, requiring the selection of a nondiagonal $V_{+1}(z^{-1})$. When the process is not invertible, an even more difficult selection of a nondiagonal $V_{+2}(z^{-1})$ is required. An easy approach to designing IMC inverses that are optimal for the quadratic performance index, Eq. 2, would be to use the spectral factorization inverses (Kozub and MacGregor, 1987).

Table 1. Comparison of LQ and IMC Controller Designs

	IMC	LQ
$G_c(z^{-1})$:	$(\delta(z^{-1})\omega(z^{-1})^{-1}z^{k})\ V_{+1}(z^{-1})\ V_{+2}(z^{-1})$	$\delta(z^{-1})\Gamma(z^{-1})^{-1}$
$F(z^{-1})$:	diagonal $\{(1-f_{ii})/(1-f_{ii}z^{-1})\}$	$Q\Gamma(z^{-1})\ \theta(z^{-1})^{-1}$

The exact physical meaning of the filters in the LQ design is not entirely clear, but may be interpreted as optimal prediction filters for disturbances and set-point changes corresponding to Eq. 2, and can be observed in Eq. 8 to be a function of the process model, the disturbance model, and the weighting matrices. In the minimum variance, single-input/single-output case ($Q_2 = 0$) the filters provide the minimum mean square error forecasts of $N(t)$ and $Y_{sp}(t)$ at $t + k$. In the approach of Garcia and Morari, a diagonal first-order exponential filter is arbitrarily specified and all tuning is performed using this filter block. The purpose of the filter block in this design is to reduce the bandwidth of the complementary sensitivity matrix $G_m(z^{-1})\ G_c(z^{-1})\ F(z^{-1})$. According to Doyle and Stein (1981), this will improve the robustness of the control design to model mismatch, which usually predominates in the high-frequency range. The bandwidth of the complementary sensitivity function in the LQ design is affected indirectly by Q_2 through its effect on $G_c(z^{-1})$ and $F(z^{-1})$ (Harris and MacGregor, 1987). One advantage of the IMC approach is that the filter constants can be directly adjusted on-line to tune the controller, while in the LQ approach, the controller design must be recomputed for any new value of Q_2.

Pilot Plant Reactor System

The process under investigation is a pilot plant packed-bed reactor carrying out highly exothermic butane hydrogenolysis

reactions over a nickel on silica gel catalyst. The hydrogenolysis of butane can be represented by the following overall reactions:

$$C_4H_{10} + H_2 \rightarrow C_3H_8 + CH_4$$
$$C_4H_{10} + H_2 \rightarrow 2C_2H_6$$
$$C_3H_8 + H_2 \rightarrow C_2H_6 + CH_4$$
$$C_2H_6 + H_2 \rightarrow 2CH_4 \qquad (12)$$

Only three of the reactions shown above are stoichiometrically independent, but in the usual operating region of the reactor only two are practically independent (MacGregor and Wong, 1980). Therefore, only two output or product species need to be controlled.

The reactor consists of a 3.81 cm schedule 80 stainless steel pipe mounted concentrically within a carbon steel pipe. The inner pipe contains the catalyst bed and the outer pipe forms a cooling jacket for a heat transfer oil circulation loop. The length of the catalyst bed is 89 cm. The feed gases, hydrogen and butane, are mixed upstream and enter the reactor with back pressure set at 97 kPa. Thermocouples positioned on the axis of the reactor provide temperature profile readings along the length of the bed. The region of operation is set by maintaining a constant wall-temperature set point. On/off control of an air source to a shell-and-tube heat exchanger in the oil circulation loop is used to regulate wall temperature. An on-line gas chromatograph system sampling the effluent provides concentration measurements at 3 min intervals.

The process control configuration of the pilot plant is shown in Figure 2. Percent butane conversion and propane production (cm^3/s) are the outputs controlled by a multivariable outer loop controller that computes control actions at 3 min intervals from the gas chromatograph readings. The multivariable control inputs are hydrogen flow rate set point (cm^3/s) and hot-spot set point (°C). Hot-spot set point is sent to an internal hot-spot control loop that uses the butane flow rate set point to control the difference between the reactor wall temperature set point and the hottest temperature detected by the thermocouples in the bed. Control actions are taken by the hot-spot loop at 30 s intervals. Temperature gradients exist in the reactor bed due to the highly exothermic reactions and the limited ability to remove heat from the center of the reactor through the reactor wall. A typical temperature profile along the axis of the bed is given in Figure 3. The purpose of the internal hot-spot loop is to provide a safe open-loop stable configuration for multivariable control.

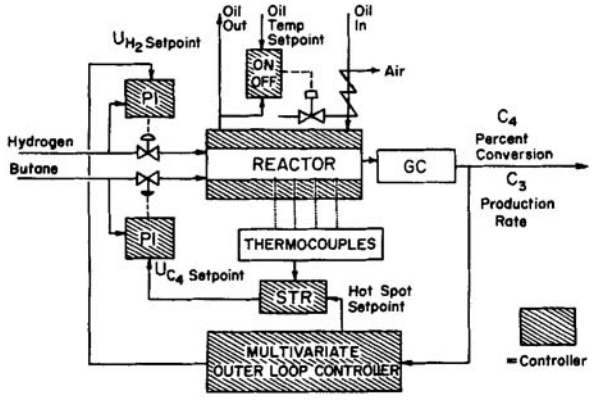

Figure 2. Control configuration.

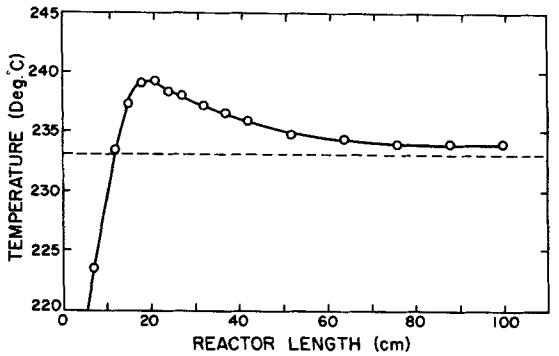

Figure 3. Axial temperature profile, wall temperature = 233°C.

Hydrogen and butane flow rate set points are determined by the multivariable control loop and the hot-spot inner loop, respectively. The flow rates of the two feed streams are controlled every second by discrete PI controllers.

The hot-spot temperature controller is a one-step optimal LQ controller tuned by using the implicit self-tuned controller of Clarke and Gawthrop (1975). The self-tuning approach was used simply as a convenient way to tune the temperature controller; it was not used in a continuously adaptive mode. Since the response of hot-spot temperature change to change in butane flow rate is very nonlinear, a logarithmic transformation of the hot-spot temperature was used to linearize the temperature control loop. The controlled output after the linearizing transformation becomes

$$Y(t) = \ln[\text{hot-spot}(t)] - \ln[\text{hot-spot set point}(t)] \qquad (13)$$

where

$$\text{hot-spot}(t) = \text{hot-spot temperature}(t) - \text{wall temperature}(t) \qquad (14)$$

This nonlinear transformation was found to greatly improve the performance of the self-tuning regulator. The choice of the input magnitude constraint factor in the one-step optimal algorithm was used to provide a trade-off between acceptable hot-spot control to stabilize the system and the requirement of smooth variations of the butane feed rate. The second requirement was necessary since the end objective was to control the reactor output production rates rather than hot-spot temperature. Details of this controller design are given by Onderwater et al. (1987).

The pilot plant is operated through a distributed control network. The computer hardware consists of a Digital Equipment Corporation VAX11/750 host computer connected to a DPM-23 Front End minicomputer. A Varian VISTA 6000 gas chromatograph (GC) and a Varian VISTA 401 CG control station are interfaced to the computer hardware. Communication between the user and the field is handled by real-time software running in both the VAX11/750 and the DPM-23. Input/output and low-level control operations are performed in the DPM-23 Front End while high-level control, operator communication, and data logging are performed by the VAX host.

Model Identification

A theoretical investigation of the process using fundamental material and energy balances can be performed to develop a

mechanistic dynamic model. Jutan (1976) has shown that this will lead to four simultaneous, nonlinear partial differential equations. Detailed knowledge of the reaction kinetics and process parameters together with lengthy mathematical model reduction operations is required to arrive at a usable model for control.

In this work an empirical transfer function approach was selected to model the dynamics of the system based on input/output data. This technique eliminates the very substantial effort required to develop a mechanistic model at the expense of losing some important insight into the process. Multivariable time series analysis combined with process identification techniques was used to develop an empirical linear model. The details of this identification technique are covered in depth by Wilson (1970) and Box and Jenkins (1976). This approach was used to identify a linear transfer function and disturbance model that approximates the dynamics of the process in the region of operation.

Dynamic data were generated by pseudorandom binary sequence (PRBS) perturbations of the input variables and discrete sampling of the reactor temperatures and product composition. Hydrogen flow rate was switched between 68 and 83 cm^3/s. Hot-spot set point was switched between 5 and 9°C above the wall-temperature set point. Wall-temperature set point was kept constant at 232°C during the data gathering. Two PRBS switching periods (6 and 18 min) were used in the identification run to allow for efficient identification of both the fast and slow modes of the process. From previous studies it was found that the concentration dynamics had time constants of the order of 10 s, whereas the thermal time constants were approximately 20 min.

The input/output time series data were used to identify a model in the canonical form

$$Y(t) = V(z^{-1})U(t) + N(t) \tag{15}$$

$$\Phi(z^{-1})N(t) = \Theta(z^{-1})A(t) \tag{16}$$

where

$V(z^{-1})$ is an $n \times n$ rational polynomial matrix in z^{-1}

$\Phi(z^{-1})$ is an $n \times n$ diagonal polynomial matrix in z^{-1} having nonrational elements and z^0 coefficient equal to I

$\Theta(z^{-1})$ is a full $n \times n$ polynomial matrix in z^{-1} having nonrational elements and z^0 coefficient equal to I

Maximum likelihood parameter estimation and statistical diagnostic checking procedures led to the approximate linear model

$$Y(t) = \begin{bmatrix} \dfrac{1.8 - 6.643z^{-1} + 5.158z^{-2}}{1 - 1.04z^{-1} + 0.3412z^{-2}} & \dfrac{0.5384z^{-1}}{1 - 1.262z^{-1} + 0.5203z^{-2}} \\ -0.7498 - 3.398z^{-1} - 1.012z^{-2} & \dfrac{0.1592z^{-2} + 0.1143z^{-3}}{1 - 0.6143z^{-1}} \end{bmatrix} U(t-3) + \begin{bmatrix} 1 + 0.126z^{-1} & -0.1249z^{-1} \\ 0.2112z^{-1} & 1 - 0.3904z^{-1} \end{bmatrix} \begin{bmatrix} (1 - z^{-1}) & 0 \\ 0 & (1 - z^{-1}) \end{bmatrix}^{-1} A(t) \tag{17}$$

where

$Y_1(t)$ = (propane production − 24) mmol/s

$Y_2(t)$ = (butane conversion − 29.6) %

$U_1(t)$ = (hydrogen flow rate − 75) $cm^3/s \times 10^{-1}$

$U_2(t)$ = (hot-spot set point − 7) °C

and the covariance matrix for the innovations $A(t]$ was

$$\Sigma = \begin{bmatrix} 0.134 & 0.043 \\ 0.043 & 0.200 \end{bmatrix} \tag{18}$$

The design of a controller for this interactive process model is far from trivial. The process model can be shown to display an initial wrong-way propane production response with respect to changes in hydrogen flow rate. The model contains one nonminimum phase zero located at (−5.5, 0.0), and a stable ringing zero located at (−0.58, 0.0). One period of time delay imbalance is also present.

Previous identification studies by Onderwater (1985) showed evidence of a fairly high degree of dynamic nonlinearity over the wide range of outputs and inputs to be considered. Steady state gains were observed to vary up to a factor of four in the transfer functions identified at different operating conditions. Approximately the same range of variation in the time constants was also observed. These variations result mainly from the highly nonlinear temperature and concentration dependence of the reaction rates over the operating space of the reactor. Significant dynamic nonlinearities were also present at nominal operating conditions, mainly due to the effect of the control inputs on the internal hotspot temperature control loop. Another source of process model mismatch was due to catalyst activity changes. An investigation by Yang (1982), revealed that changes in the catalyst activity by a factor of two were possible between successive runs. Therefore, the linear process transfer function could only be considered to be a rough linear approximation to the true process dynamics, and in the design of the controllers robustness to process/model mismatch was an important consideration.

The nonstationary stochastic disturbance model identified for this process is characteristic of processes displaying drift in level with superimposed white measurement noise (Box and Jenkins, 1976). The open-loop performance of the reactor with only the internal hot-spot control loop active is shown in Figure 4. In this run the hydrogen flow rate set point and the hot-spot set point were fixed at 75 cm^3/s and 7°C, respectively. The nonstationarity of the process outputs can be observed particularly in the butane conversion, where drifts of up to 7% can be seen. In the following controller designs both regulation of these stochastic

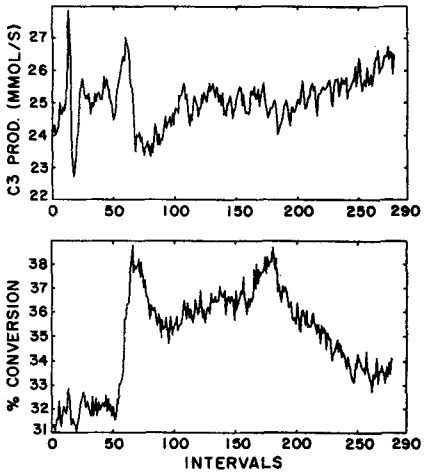

Figure 4. Open-loop output data.
Top, propane production rate
Bottom, % butane conversion

disturbances and good servo response to step changes in set point are considered.

Control Studies

LQ and IMC controllers were designed using the model transformed into the right matrix fraction form. The control objective for both designs was to achieve good stable regulatory and servo performance, while at the same time minimizing the variations in the input manipulations required to achieve this control. Adequate robustness to the large degree of process/model mismatch that exists over the operating region of the reactor was required.

Formal approaches to addressing the problem of controller robustness, such as the use of singular values or principle gains for assessing the effect of unstructured uncertainty (Doyle and Stein, 1981), and structured singular-value methods (Doyle, 1982), have been widely advocated in recent years. However, these methods require that the designer possess considerable knowledge about the nature and the magnitude of model uncertainties. For multivariable, nonlinear systems such as catalytic reactors this type of knowledge is difficult to obtain, and might only be reasonably obtained through developing a detailed mechanistic model, or by performing extensive plant experimentation with a wide range of operating conditions, catalyst activities, etc. In this study, a preliminary analysis of controller robustness was made using the singular-value approach of Doyle and Stein. Transfer functions identified by Onderwater (1985) for the reactor at different operating conditions were used to provide an envelope for possible model mismatch in the frequency domain. However, this procedure proved to be far too conservative to provide any useful *a priori* robustness guarantees. It even appeared to be unable to predict adequately the relative robustness of the different controllers.

Therefore, an indirect approach to addressing controller robustness was taken in this study. The controller tuning parameters, Q_2 for the LQ controllers and filter constants f_{ii} for the decoupled IMC controller, were adjusted to provide a reasonable compromise between the output performance achieved with the nominal model, Eq. 17, and the amount of input variation necessary to achieve it. Intuitively, by taking less severe control actions one would expect more robust control. Furthermore, as elements of Q_2 and f_{ii} are increased the bandwidth of the closed-loop system is decreased, making it generally less sensitive to high-frequency modeling errors. Control simulations were performed to evaluate these controllers against both the nominal model, Eq. 17, and various alternative models (Onderwater, 1985). These preliminary designs were then implemented on the pilot plant reactor, and based on the observed performance further tuning was achieved by varying the elements of Q_2 or the filter parameters f_{ii}. The ultimate evaluation of the performance and robustness of the controllers was then obtained by observing their behavior over the entire operating space of the experimental reactor.

LQ controller design

The LQ controller was to be designed to compensate for the identified nonstationary stochastic disturbances and to accommodate step changes in the set points of either output. The model for randomly occurring step changes in set points is given by

$$\nabla Y_{sp}(t) = a(t) \tag{19}$$

where $\nabla = (1 - z^{-1})I$. Since the structure of this model for set point changes is very close to that for the stochastic disturbances in the process model, Eq. 17, it was considered sufficient to design the LQ controller for the disturbance model in Eq. 17 and take $F_1(z^{-1}) = F_2(z^{-1})$ in the controller given by Eqs. 3, 4, and 5. This of course would be exactly correct if the disturbance model were identical to the set point change model (Harris and MacGregor, 1987). The LQ controller used was, therefore, the single degree of freedom controller

$$U(t) = H_1(z^{-1})\{G_m(z^{-1})U(t) - [Y(t) - Y_{sp}(t)]\} \tag{20}$$

The form of the cost function, Eq. 2, and the disturbance model in Eq. 17 leads to a controller containing integral action in both outputs. The output weighting matrix Q_1 was set to I for all controller designs and Q_2 was adjusted to provide the required amount of input constraint and controller robustness.

The matrix spectral factors $\Gamma(z^{-1})$ and $T(z^{-1})$ matrices corresponding to the different choices of input weighting matrices used in this study are listed in the Appendix. The particular disturbance model used in this study leads to a constant, zero-order $T(z^{-1})$ matrix. Hence the filter block is fixed in the LQ design, unaffected by the selection of weighting matrices. Tuning with the Q_2 input weighting matrix only has an effect on the approximate model inverse $G_c(z^{-1})$. It is interesting to note that the structure of the filter in the LQ controller is a first-order exponential filter like that used in the IMC design below except that the filter matrix is not diagonal, as a result of the interactive nature of the disturbance model. This nondiagonal filter, and the fact that spectral factorization inverse is such that $G_m(z^{-1})G_c(z^{-1})F(z^{-1})$ is not diagonal, means that this LQ controller does not yield a decoupled system (see discussion in Harris and MacGregor, 1987).

Decoupled IMC design

An IMC controller leading to a decoupled response with the nominal model was designed using the method described earlier.

The decoupled design is suboptimal in terms of integrated square error because the process model is nonminimum phase and not balanced with respect to time delays. A stable model inverse $G_c(z^{-1})$ was selected according to Eq. 10 with $V_{+1}(z^{-1})$ and $V_{+2}(z^{-1})$ taken to be diagonal matrices

$$V_{+1}(z^{-1}) = \begin{bmatrix} z^{-4} & 0 \\ 0 & z^{-4} \end{bmatrix} \tag{21}$$

and

$$V_{+2}(z^{-1}) = \frac{(1 + 5.51z^{-1})(1 + 0.58z^{-1})}{(5.51 + z^{-1})(1.58)} I \tag{22}$$

This $G_c(z^{-1})$ design leads to the closed-loop response

$$Y(t) = N(t) + \frac{z^{-4}(1 + 5.51z^{-1})(1 + 0.58z^{-1})}{(5.51 + z^{-1})(1.58)} \cdot F(z^{-1})[Y_{SP}(t) - N(t)] \tag{23}$$

with the nominal model. $V_{+1}(z^{-1})$ was used to make the controller realizable. This choice of $V_{+1}(z^{-1})$ leads to four periods of delay in the closed-loop output response. The nonminimum phase zero and the ringing zero were removed with $V_{+2}(z^{-1})$, and the uncancelled dynamics associated with these zeros will therefore appear in the closed-loop responses of both outputs. The unstable zero at $(-5.51, 0)$ was replaced by its image inside the unit circle, and the ringing zero at $(-0.58, 0)$ was moved to the origin.

The same $G_c(z^{-1})$ was used in all of the IMC designs, and tuning adjustments were made through the diagonal first-order exponential filter block.

Controller simulation

Simulations with the identified nominal process and disturbance model, Eq. 17, were performed to compare controllers and to determine reasonable starting tuning parameters for implementation on the pilot plant process. Identical disturbance and set point change sequences were made in all of these simulated control runs. The sequence of set point changes made was similar to those used in the actual experimental runs, Figures 5–10.

The simulated performance of two different LQ controllers, two decoupled IMC controllers, and two PI controllers has been summarized in Table 2 for both regulation and servo response to the same sequence of step changes in set points. The performances are evaluated in terms of output error variance and variance of the input changes required to achieve that control. As expected, the LQ controller design with $Q_2 = 0$ leads to the lowest output variances. However, the variances of $\nabla U(t)$ indicate that this design also calls for very large input manipulations, making it unacceptable for implementation. The LQ controller designed with input weighting matrix $Q_2 =$ diag (100, 10) leads to a very significant reduction in the variance of $\nabla U(t)$, and yet the loss in output performance is only slight. Because of the reduction of the input variance, one would expect this controller to be much more robust than the first LQ design (Harris and McGregor, 1987), and therefore it was considered reasonable for actual implementation.

The decoupled IMC design without filtering leads to slightly poorer simulated output performance relative to the LQ design with $Q_2 = 0$. It also leads to very large $\nabla U(t)$ variances, making it unacceptable for implementation. The filter parameters in the tunable filter block were increased to diag (0.7, 0.7) to reduce the variance of the input manipulations and to improve robustness. These filter parameters were considered to be reasonable initial choices for actual implementation. Note that the detuned IMC design led to larger total variances of both the outputs and the input changes relative to the detuned LQ design.

Table 2. Simulated Controller Performance for Set-point Changes and Disturbance Regulation

Controller Design	Variances: Propane Prod.	Butane Conv.	H_2 Flow Changes	Hot-spot Changes
LQ: $Q_1 = I$, $Q_2 = 0$	3.044	2.319	1.6	7.081
LQ: $Q_1 = I$, $Q_2 =$ diag (100,10)	3.411	2.498	0.4	0.044
Decoupled IMC $f_{11} = f_{22} = 0.0$	3.155	2.56	1.6	2.576
Decoupled IMC $f_{11} = f_{22} = 0.7$	3.964	3.195	0.3	0.137
PI: Zeigler-Nichols	6.221	2.984	5.6	0.009
PI: Improved settings $K_{c12} = 0.05$; $K_{c21} = -0.03$ $\tau_{I12} = 3$ min; $\tau_{I21} = 5$ min	4.975	3.061	1.6	0.002

Simulated controller performance for two different PI designs with paired inputs has been included in Table 2 to compare the performance of the multivariable controller designs with conventional single-loop design methods. It was determined that pairing hot-spot set point with propane production and hydrogen flow rate set point with conversion would lead to the most effective multiloop design. The first set of PI controllers was designed using Zeigler-Nichols suggested settings. These tuning settings led to very poor control of the propane production rate. An extensive trial and error search was made to arrive at a second set of tuning parameters leading to improved output performance. It is clear that both multivariable designs provide superior control.

Experimental LQ control runs

Figure 5 shows an experimental control run on the pilot plant reactor with the same catalyst charge used during the model identification studies. An input constraint matrix of $Q_2 =$ diag (100, 10) was selected for this run. The dashed lines in Figure 5 indicate operating set points and the dotted lines indicate the measured outputs. The abscissa in these figures and on those that follow refers to the sampling interval, where each sampling interval represents 3 min. The solid line of the bottom, input setting portion of the figure represents the hydrogen flow rate set point ($cm^3/s \times 10^{-1}$) and the dashed line represents the hot-spot set point (°C). Excellent regulation can be observed in the first 5 h section of data in this run. In the remaining part of the run a variety of conversion and propane production rate set point changes were made, some in the same direction, some in opposite directions, and some where only one set point was changed. In all cases the set point change performance of the controller

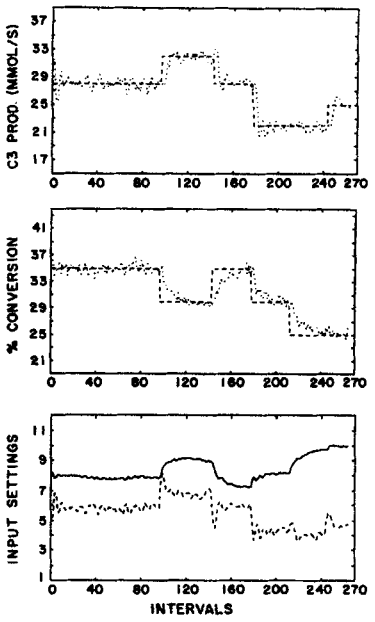

Figure 5. Experimental LQ control run, old catalyst charge.

$Q_1 = I$; Q_2 = diag (100, 10)
Top, ····· propane production rate; --- set point
Middle, ····· % butane conversion; --- set point
Bottom, — hydrogen flow rate; --- hot-spot temperature rise

was good, and it appeared to be robust over the wide range of operating conditions studied. No significant closed-loop interaction can be observed when the final two set point changes were made where one of the two set points was held fixed. Figure 5 shows that input manipulations were smooth and well-behaved during the entire control run.

Figure 6 shows a control run using the same Q_2 = diag (100, 10) but with a new catalyst charge in the reactor. The outputs, especially percent conversion, are noticeably noisier than those in Figure 5. During operation with this new charge it was noticed that an oil leak was present in the system, resulting in a catalyst activity decay at the entrance of the bed due to poisoning. However, regulation and set point change performance was still good over the whole range of the operation.

A more tightly tuned LQ control run with less constraint on the input variances, using Q_2 = diag (50, 5) is shown in Figure 7. This control run was also performed with a higher wall temperature of 233°C (vs. 232°C in Figures 5 and 6) and all set points were raised five units relative to the previous run. The adjustment was made to compensate for a significant shift in the location of the reactor hot-spot temperature relative to the conditions in the previous runs. During this run, the input manipulations and the rate of propane production displayed a high degree of oscillation. The problem became more severe when a set point change was made to a region of low propane production and high conversion. The poorer performance relative to the previous run can be attributed to a decrease in the controller robustness due to the tighter tuning (smaller Q_2), which made the controller sensitive to process/model mismatch caused by the significant change in operating conditions and the reactor nonlinearities.

The experimental performance of these controllers during stable regulation at the different operating levels is summarized in Table 3. The table gives controller performance in terms of the variance of output deviations from their set points. The output variance of the open-loop run shown in Figure 4 has been included for comparative purposes. Relative to the open-loop data, the LQ controller designed with Q_2 = diag (100, 10) led to a significant reduction in output variance using both the new and old catalyst charge. This was not true for the LQ controller designed with Q_2 = diag (50, 5) where a larger propane production variance can be observed compared to the open-loop run.

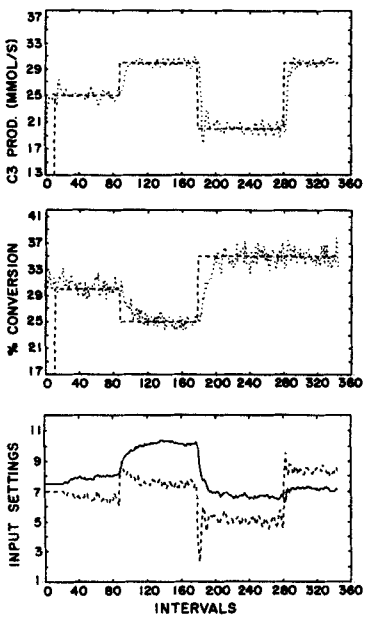

Figure 6. Experimental LQ control run, new catalyst charge.

Q_2 = diag (100, 10)
Curve identification as in Figure 5

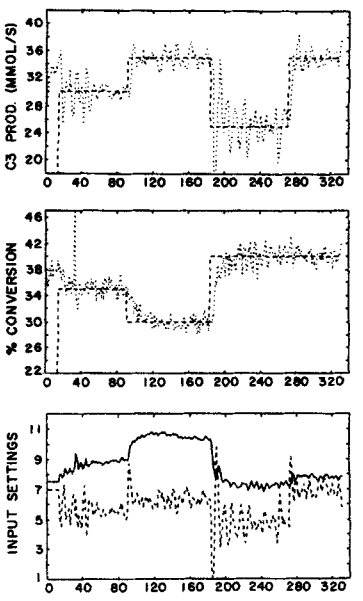

Figure 7. Experimental LQ control run, new catalyst charge.

Q_2 = diag (50, 5)
Curve identification as in Figure 5

Table 3. Experimental Performance of Controllers During Regulation

Controller	Variance: Propane Production Rate	Variance: Butane Conversion %
Open-loop	0.58	3.84
LQ: Q_2 = diag {100,10} Old catalyst	0.32	0.27
LQ: Q_2 = diag {100,10} New catalyst	0.31	0.95
LQ: Q_2 = diag {50,5} New catalyst (high set points)	1.54	1.04
IMC: f_{ii} = {0.7,0.7} New catalyst	0.44	0.84
IMC: f_{ii} = {0.9,0.8} New catalyst (high set points)	0.50	0.98
IMC: f_{ii} = {0.9,0.9} New catalyst	0.58	1.13

Experimental IMC runs

A decoupled IMC control run with the filter constants f_{ii} tuned to diag (0.7, 0.7) is shown in Figure 8. This run was performed immediately following the LQ run in Figure 6 with the new catalyst charge. The identical pattern of set point changes was made in all of these runs in order to facilitate comparisons. Set point change performance and regulation were good for the first two set points. The second set point change demanding high conversion with low propane production led to very poor controller performance. Large oscillations observed with the inputs and propane production suggest controller instability in this region of operation. Complete recovery by the controller can be seen when a set point change was made in propane production rate back to a more stable region of operation.

In order to increase the robustness of this IMC controller to accommodate such set point changes, the controller was detuned by using larger filter constants in $F(z^{-1})$, namely F = diag (0.9, 0.9). The control run is shown in Figure 9. Detuning led to substantial reduction in the variation of the input manipulations. Regulation still appeared to be good over the full region of operation. Improved robustness to the process nonlinearities can be observed by the stable controller performance when the set-point changes were made to the region of high conversion and low propane production. No significant interaction was observed when the final set point change was made to propane production with conversion set point held fixed.

The filter block was retuned to improve the sluggish set point change response of butane conversion. A control run with F = diag (0.9, 0.8) is shown in Figure 10. This control run was performed at a higher wall temperature of 233°C to compensate for a significant shift in the location of the reactor hot-spot temperature, and all set points were shifted five units higher relative to the previous runs. Again, regulation was adequate over the entire region of operation although slightly increased deviation of propane production was observed in the region of low propane production and high butane conversion. Substantial improvement in the set point change response of butane conversion can be observed in Figure 10 relative to the previous controller, as a result of the smaller filter constant (0.8 vs. 0.9).

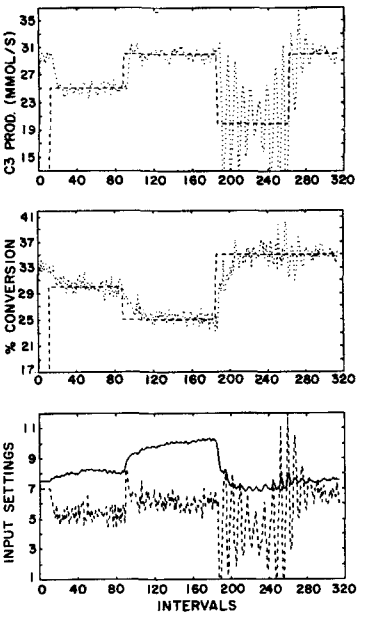

Figure 8. Experimental IMC control run, new catalyst charge.
F = diag (0.7, 0.7)
Curve identification as in Figure 5

The experimental performance of the decoupled IMC controller design during the periods of regulation is also listed in Table 3. The period of unstable regulation at low propane production rate and high conversion using the IMC controller tuned with filter constants f_{ii} = diag (0.7, 0.7) has been excluded in the analysis. The IMC controller with the filter constants f_{ii} tuned to

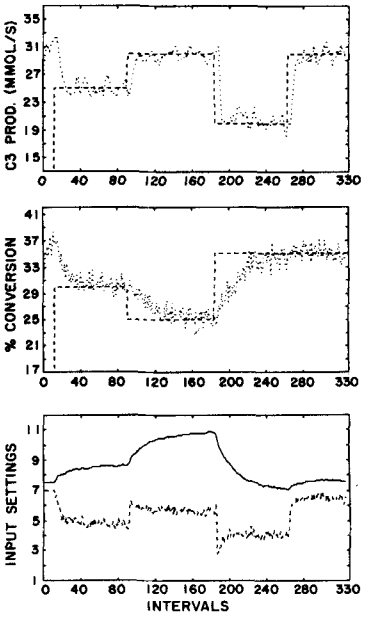

Figure 9. Experimental IMC control run, new catalyst charge.
F = diag (0.9, 0.9)
Curve identification as in Figure 5

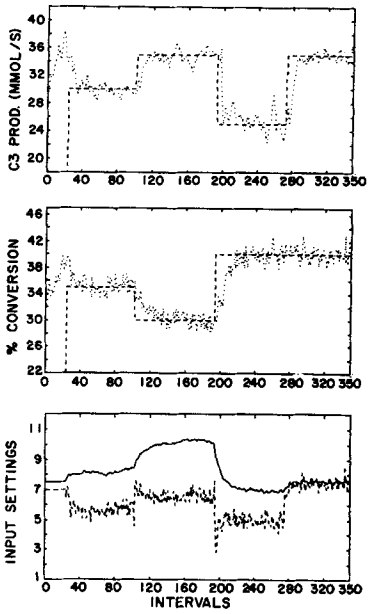

Figure 10. Experimental IMC control run, new catalyst charge.

F = diag (0.9, 0.8)
Curve identification as in Figure 5

diag (0.7, 0.7) displays significant improvement in output variance compared to the open-loop data. As expected, output error variance can be seen to increase with the larger filter constants. Detuning the filter parameters to F = diag (0.9, 0.9) led to no improvement in the variance of propane production during regulation relative to the open-loop data, although significant improvement can still be seen in the variance of percent butane conversion.

Conclusions

An application of LQ and decoupled IMC designs to composition control of a packed-bed butane hydrogenolysis reactor was considered to be very successful. An experimentally identified pulse transfer function model was used in these designs. Both multivariable designs, when well tuned, were robust to process nonlinearities and provided good regulatory and servo control over a wide region of operation.

The results indicate that the tightness of control for both controller designs was restricted by severe model mismatch, mainly due to process nonlinearities and changing catalyst properties. However, adjustment of the tuning matrices led to robust designs with acceptable regulation and set point change performance. Further improvement in the performance of these controllers would require use of adaptive control, or a nonlinear model in the $G_m(z^{-1})$ block to eliminate some of the significant nonlinear and time-varying sources of model mismatch.

Acknowledgment

The authors thank the Natural Science and Engineering Research Council of Canada for support of this research.

Notation

$A(t)$ = white noise vector
$e(t)$ = output error from set point
E = expectation
f_{ii} = first-order exponential filter factor of output i
$F(z^{-1})$ = filter block
$F_1(z^{-1})$ = disturbance filter
$F_2(z^{-1})$ = set-point filter
$G_c(z^{-1})$ = approximate model inverse in IMC design
$G_m(z^{-1})$ = nominal linear process matrix transfer function
$G_p(z^{-1})$ = true process matrix transfer function
$H_1(z^{-1})$ = product of $G_c(z^{-1})$ and $F_1(z^{-1})$, Eq. 4
$H_2(z^{-1})$ = product of $G_c(z^{-1})$ and $F_2(z^{-1})$, Eq. 5
J = quadratic cost function
k = periods of deadtime in $G_m(z^{-1})$
k_c = proportional controller gain in PI controller
n = number of inputs/outputs
N = horizon in quadratic cost function
$N(t)$ = disturbance vector
$P(z)$ = matrix polynomial in Diophantine Eq. 9
Q_1 = output penality weight matrix in LQ design
Q_2 = input penality weight matrix in LQ design
$s(j)$ = maximum positive power of z in row j of $\omega(z^{-1})^{-1} z^k$
t = sampling interval
$T(z^{-1})$ = matrix polynomial in Diophantine Eq. 9
$U(t)$ = input vector
$V_{+1}(z^{-1})$ = matrix factor to make model inverse realizable in $G_c(z^{-1})$ for IMC design
$V_{+2}(z^{-1})$ = matrix factor to replace zeros of model inverse in $G_c(z^{-1})$ for IMC design
$Y(t)$ = output vector
$Y_{sp}(t)$ = output set point vector
z^{-1} = backward shift operator

Greek letters

$\alpha(t)$ = vector of innovations
$\Gamma(z^{-1})$ = matrix special factor, Eq. 7
$\delta(z^{-1})$ = diagonal polynomial matrix in process transfer function, Eq. 1
∇ = backward difference operator
$\theta(z^{-1})$ = nonrational matrix in ARIMA disturbance model, Eq. 1
Σ = covariance matrix of $A(t)$
τ_I = integral time in PI controller
$\phi(z^{-1})$ = diagonal polynomial matrix in ARIMA disturbance model, Eq. 1
$\omega(z^{-1})$ = polynomial matrix in process transfer function, Eq. 1

Appendix: LQ Controller Designs

$G_c(z^{-1})$ designs

$$G_c(z^{-1}) = \delta(z^{-1})\Gamma(z^{-1})^{-1}$$

$$\delta(z^{-1}) = \begin{bmatrix} 1 - 1.04z^{-1} + 0.3412z^{-2} & 0 \\ 0 & 1 - 1.876z^{-1} + 1.296z^{-2} - 0.3196z^{-3} \end{bmatrix}$$

a)

$$Q_1 = I \quad Q_2 = 0$$

$$\Gamma(z^{-1}) = \begin{bmatrix} -2.74 & 0.496 \\ -5.59 & 0.230 \end{bmatrix} + \begin{bmatrix} 2.22 & -0.241 \\ 6.24 & -0.240 \end{bmatrix} z^{-1} + \begin{bmatrix} 0.686 & -0.084 \\ -1.858 & 0.094 \end{bmatrix} z^{-2} + \begin{bmatrix} 0.119 & 0.055 \\ -0.291 & -0.061 \end{bmatrix} z^{-3} + \begin{bmatrix} 0.028 & -0.014 \\ -0.06 & 0.036 \end{bmatrix} z^{-4} + \begin{bmatrix} 0 & -0.005 \\ 0 & 0.010 \end{bmatrix} z^{-5}$$

b)

$$Q_1 = I \quad Q_2 = \text{diag}\,(100, 10)$$

$$\Gamma(z^{-1}) = \begin{bmatrix} -2.76 & 4.02 \\ -13.35 & -0.513 \end{bmatrix} + \begin{bmatrix} 4.6 & -9.59 \\ 21.21 & 1.748 \end{bmatrix} z^{-1} + \begin{bmatrix} -1.83 & 9.28 \\ -11.8 & -1.91 \end{bmatrix} z^{-2} + \begin{bmatrix} 0.307 & -4.27 \\ 2.389 & 0.88 \end{bmatrix} z^{-3} + \begin{bmatrix} -0.0024 & 0.776 \\ -0.018 & -0.147 \end{bmatrix} z^{-4} + \begin{bmatrix} 0 & 0.0004 \\ 0 & 0.0032 \end{bmatrix} z^{-5}$$

c)

$$Q_1 = I \quad Q_2 = \text{diag}\,(50, 5)$$

$$\Gamma(z^{-1}) = \begin{bmatrix} -3.02 & 3.01 \\ -10.48 & -0.513 \end{bmatrix} + \begin{bmatrix} 4.71 & -6.78 \\ 15.42 & 1.70 \end{bmatrix} z^{-1} + \begin{bmatrix} -1.62 & 6.32 \\ -7.89 & -1.82 \end{bmatrix} z^{-2} + \begin{bmatrix} 0.25 & -2.84 \\ 1.42 & 0.82 \end{bmatrix} z^{-3} + \begin{bmatrix} -0.004 & 0.51 \\ -0.023 & -0.13 \end{bmatrix} z^{-4} + \begin{bmatrix} 0 & 0.0007 \\ 0 & 0.0040 \end{bmatrix} z^{-5}$$

$F(z^{-1})$ design

$$F(z^{-1}) = T(z^{-1})\theta(z^{-1})^{-1}$$

$$T(z^{-1}) = \begin{bmatrix} 1.126 & -0.125 \\ 0.211 & 0.609 \end{bmatrix}$$

$$F(z^{-1}) = \begin{bmatrix} 1.126 & -0.125 \\ 0.211 & 0.609 \end{bmatrix} \begin{bmatrix} 1 + 0.126z^{-1} & -0.125z^{-1} \\ 0.211z^{-1} & 1 - 0.39z^{-1} \end{bmatrix}^{-1}$$

Literature Cited

Bergh, L. G., and J. F. MacGregor, "Constrained Minimum Variance Controllers: Internal Model Structure and Robustness Properties," *Ind. Eng. Chem. Proc., Des. Dev.* (1987); also Tech. Rept. No. 1001, Process Control Lab. ChE. Dept., McMaster Univ.

Box, G. E. P., and G. M. Jenkins, *Time Series Analysis: Forecasting and Control*. Holden-Day, San Francisco (1976).

Clarke, D. W., and P. J. Gawthrop, "Self-Tuning Controllers," *Proc. IEE*, **122**, 929 (1975).

Doyle, J. C., "Analysis of Feedback Systems with Structured Uncertainties," *IEE Proc.*, **129, D**, (6), 242 (1982).

Doyle, J. C., and G. Stein, "Multivariable Feedback Design: Concepts for a Classical/Modern Synthesis," *IEEE Trans. Auto. Control*, **AC-26**(1) (1981).

Garcia, C. E., and M. Morari, "Internal Model Control. 2: Design Procedure for Multivariable Systems," *Ind. Eng. Chem. Process Des. Dev.*, **24**, 472 (1985a).

———, "Internal Model Control. 3: Multivariable Control Law Computation and Tuning Guidelines," *Ind. Eng. Chem. Process Des. Dev.*, **24**, 484 (1985b).

Harris, T. J., and J. F. MacGregor "Design of Multivariable Linear Quadratic Controllers Using Transfer Functions," *AIChE J.* (Oct., 1987).

Holt, B. R., and M. Morari, "Design of Resilient Processing Plants. VI: The Effect of Right Half-Plane Zeros on Dynamic Resilience," *Chem. Eng. Sci.*, **40**(1), 59 (1985a).

———, "Design of Resilient Processing Plants. V: The Effect of Deadtime on Dynamic Resilience," *Chem. Eng. Sci.*, **40**(7), 1229 (1985b).

Jutan, A., "State Space Modelling with Multivariate Stochastic Control of a Pilot Packed-Bed Reactor," Ph.D. Thesis, McMaster Univ., Hamilton, Canada (1976).

Jutan, A., J.D. Wright, and J.F. MacGregor, "On-line Linear Quadratic Stochastic Control Studies," *AIChE J.*, **23**(5), 751 (1977).

Kozub, D. J., "Advanced Model-Based Multivariate Control Design and Application to Packed-Bed Reactor Control," M.Eng. Thesis, Dept. Chem. Eng., McMaster Univ. Hamilton, Canada (1986).

Kozub, D. J., and J. F. MacGregor, "Optimal IMC Inverse Design via Spectral Factorization," *Proc. 1987 Am. Control Conf.*, Minneapolis (1987).

MacGregor, J. F., and A. K. L. Wong, "Multivariate Model Identification and Stochastic Control of a Chemical Reactor," *Technometrics*, **22**(4), 453 (1980).

MacGregor, J. F., et al., "Advanced Process Control, An Intensive Short Course on Digital Computer Techniques for Process Identification and Control," McMaster Univ. Hamilton, Ontario, Canada (1984).

Onderwater, D., "Control System Configuration and Multivariable Identification of a Packed Bed Tubular Reactor," M. Eng. Thesis, McMaster Univ. (1985).

Onderwater, D., et al., "Nonlinear Temperature Control of a Catalytic Tubular Reactor Using Self-Tuning Regulators," *Can. J. Chem. Eng.* (1987). (To appear).

Sorensen, J. P., S. B. Jorgensen, and K. Clement, "Fixed-Bed Reactor Kalman Filtering and Optimal Control. I: Computational Comparisons of Discrete vs. Continuous Time Formulation," *Chem. Eng. Sci.*, **35**, 1223 (1980a).

———, "Fixed-Bed Reactor Kalman Filtering and Optimal Control. II: Experimental Investigation of Discrete-Time Case with Stochastic Disturbances," *Chem. Eng. Sci.*, **35**, 1231 (1980b).

Wallman, P. H., J. M. Silva, and A. S. Foss, "Multivariable Integral Controls for Fixed-Bed Reactors," *Ind. Eng. Chem. Fundam.*, **18**, 4, 392 (1979).

Wilson, G. T., "Modelling Linear Systems for Multivariate Control," Ph.D. Thesis, Univ. Lancaster, England (1970).

Yang, S. M., "Self-Tuning and Adaptive Control of a Pilot Plant Fluidized-Bed Reactor," M.Eng. Thesis, Ch.E. Dept., McMaster University, Hamilton, Canada (1982).

Manuscript received Aug. 25, 1986, and revision received Apr. 8, 1987.